"Green" Fabrication of High-Performance Transparent Conducting Electrodes by Blade Coating and Photonic Curing on PET for Perovskite Solar Cells

Justin C. Bonner †, Robert T. Piper †, Bishal Bhandari, Cody R. Allen, Cynthia T. Bowers, Melinda A. Ostendorf, Matthew Davis, Marisol Valdez, Mark Lee and Julia W. P. Hsu *

* Correspondence: jwhsu@utdallas.edu
† These authors contributed equally.

PET/Metal Bus Lines and Silver Nanowires

The polyethylene terephthalate (PET)/Ag metal bus line (MBL) substrate material, provided by Energy Materials Corporation, is composed of PET (100 µm thick) with Ag MBLs. MBLs were fabricated via flexographic printing of water/alcohol-based nanosilver ink on a commercial roll-to-roll (R2R) printer at 40–50 m/min. Printed features were then subjected to 20–30 s of hot air drying at 40 °C. The MBLs are roughly 30 µm wide by 120 nm tall with a center-to-center pitch of ~580 µm. The isopropyl alcohol (IPA) silver nanowire (AgNW) suspension (5 mg mL^{-1}) was purchased from Sigma-Aldrich [1], and Cheap Tubes [2]. The nominal diameter and length of Sigma-Aldrich AgNWs are 20 nm and 12 µm, respectively, while those values for Cheap Tubes AgNWs are 30 nm and 12 µm. SEM measurements of AgNWs from both vendors show an average diameter of 30 nm. A high-magnification SEM micrograph of the Sigma-Aldrich AgNWs is shown in Supplementary Figure S1a. Supplementary Figure S1b shows that AgNWs are continuous over the MBLs.

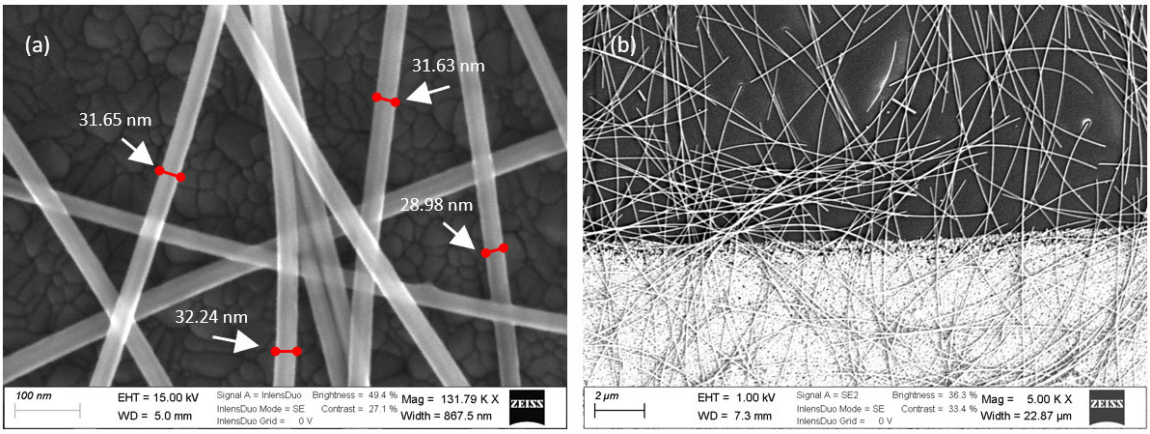

Figure S1. SEM micrographs of AgNWs: (**a**) High magnification SEM micrographs of Sigma-Aldrich AgNWs. The average diameter value from this image is 31 ± 1.5 nm. (**b**) SEM micrographs of AgNWs near an MBL.

TCE Characterization

Ultraviolet-visible (UV-Vis) transmittance spectra after each step in the hybrid TCE fabrication process is given in Supplementary Figure S2. An optical image of MBL damage after pulsing with a 5.1 J cm^{-2} pulse is shown in Supplementary Figure S3. AFM images and height profiles after AgNW deposition, one coat of IZO, and two coats of IZO are given in Supplementary Figure S4. The root mean square surface roughness (σ_{rms}) after coating with AgNW is (14.4 ± 1.0) nm, after one coat of IZO is (9.6 ± 0.9) nm, and after two coats of IZO is (4.3 ± 0.4) nm.

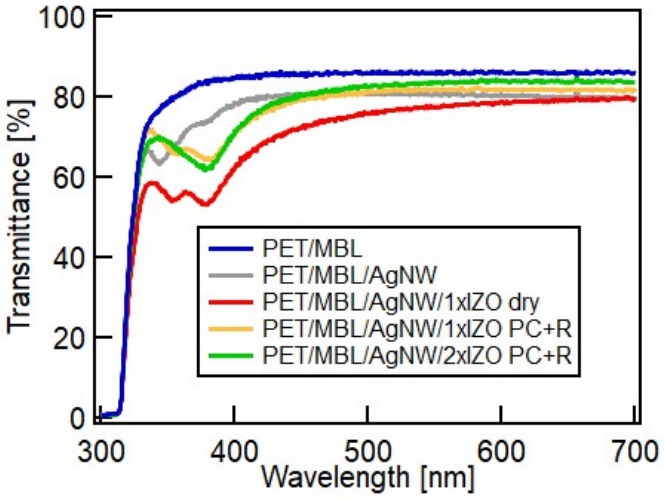

Figure S2. UV-Vis transmission of hybrid TCE: spectra referenced to air after each step in the hybrid TCE fabrication process.

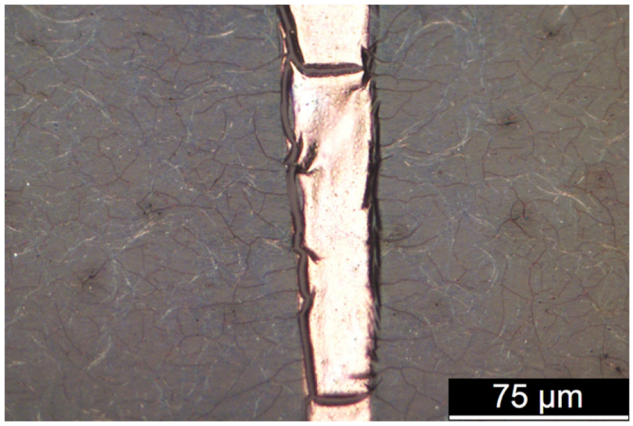

Figure S3. MBL damage after photonic curing: Optical micrographs of MBL damage resulting from a photonic curing pulse with radiant energy of 5.1 J cm^{-2}.

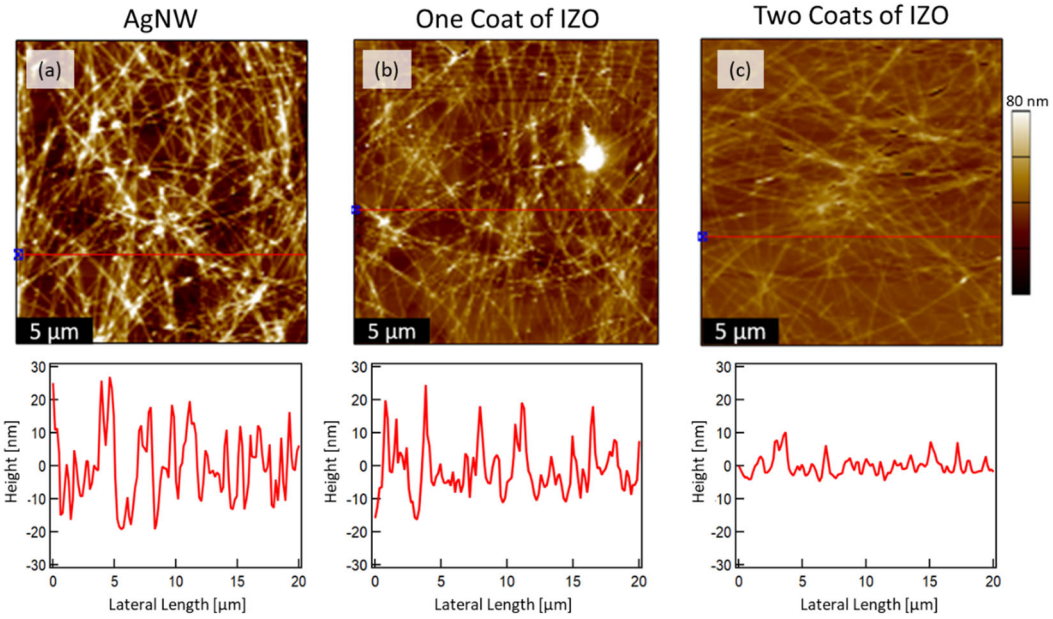

Figure S4. AFM images and height profiles of hybrid TCE: (**a**) after AgNW deposition, (**b**) after the first coat IZO, and (**c**) after the second coat of IZO on top of the PET/MBL substrates. The height profiles were taken along the red line shown in the AFM images.

The normalized XPS results for Ag 3d, In 3d, and Zn 2p are given in Supplementary Figure S5a–c. AgNWs were deposited on glass/ITO and Sigma-Aldrich PET/ITO and measured using X-ray photoelectron spectroscopy (XPS) to establish the metallic Ag binding energy of 368 eV. The binding energy for each sample spectrum was then shifted to align the Ag $3d_{5/2}$ peaks to 368 eV, as shown below in Supplementary Figure S5a.

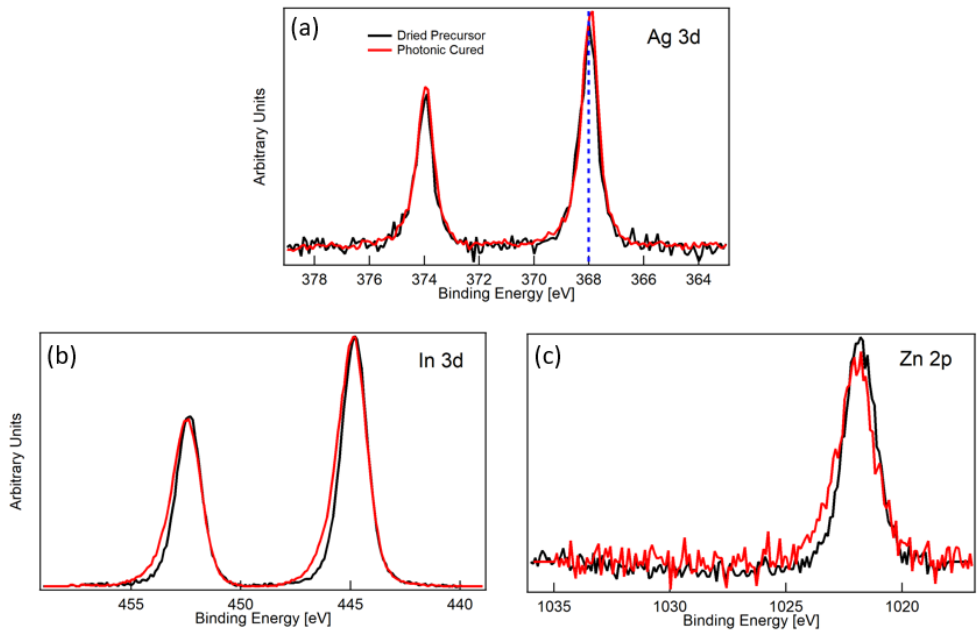

Figure S5. Normalized XPS spectra of precursor and final hybrid TCE: (**a**) Ag 3d, (**b**) In 3d, and (**c**) Zn 2p comparing the dried hybrid TCE precursor (black) and the final hybrid TCE after photonic curing (red).

Thermogravimetric analysis (TGA) was conducted with a TA Instruments Q600 on ~10 mg samples. The indium or zinc nitrate salts were placed directly in a ceramic sample pan. The temperature was ramped from room temperature to 500 °C at a ramp rate of 10 °C min^{-1} under 20 mL min^{-1} airflow. The TGA data show that indium and zinc nitrate salts completely decompose into indium or zinc oxide at ~212 °C and ~326 °C, respectively (Supplementary Figure S6).

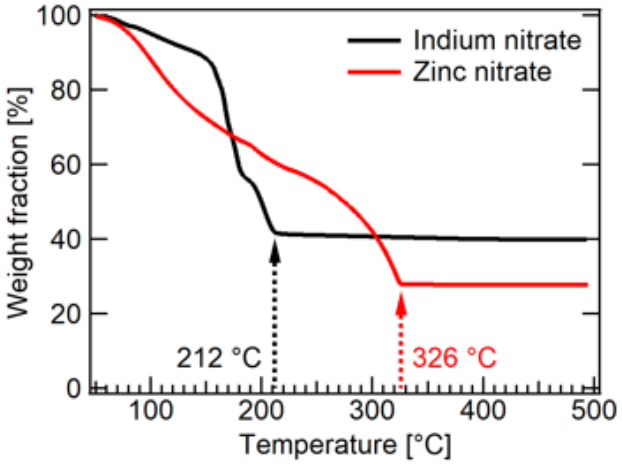

Figure S6. TGA of indium and zinc precursor salts: results of indium nitrate salt (black) and zinc nitrate salt (red).

Cross-sectional TEM image of hybrid TCE lamella prepared using a focused ion beam is shown in Supplementary Figure S7a. Supplementary Figure S7b shows a different lamella imaged using STEM away from the MBL where AgNW diameter and IZO thickness are ~26 nm and ~70 nm, respectively. The interface between the two layers of IZO can be seen in both images. It is evident that one layer of IZO is too thin to completely cover all AgNWs, explaining the roughness. Two layers of IZO are needed to uniformly overcoat the MBL and AgNWs, in agreement with Figure 2c,d and AFM images in Supplementary Figure S4.

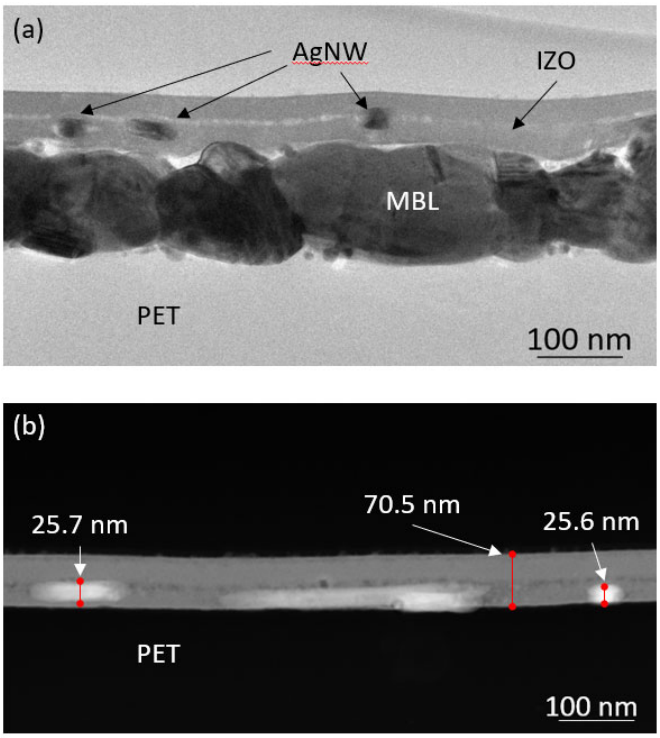

Figure S7. TEM and STEM cross section images of hybrid TCE: (**a**) TEM image of a hybrid TCE lamella taken from the MBL region, with PET, MBL, AgNWs, and IZO labeled. (**b**) STEM image of a hybrid TCE lamella taken away from the MBL. The AgNW diameters and total thickness of the two IZO coats are indicated. In both images the PET is at the bottom of the image.

To measure TCE thickness, materials are removed from hybrid TCEs by laser scribing (Supplementary Figure S8a) or by cracking the hybrid TCE and removing areas with scotch tape (Supplementary Figure S8b). To remove areas with scotch tape the hybrid TCEs were first purposely cracked by heating the sample to 120 °C. After cracking, scotch tape is applied to the top of the cracked film. Next, the sample is submerged in liquid nitrogen for up to 30 s. After taking the sample out of the liquid nitrogen, the scotch tape is carefully removed. When the tape is lifted, it also removes areas of the hybrid TCE, revealing the bare PET underneath. Now there is a step between the remaining hybrid TCE and bare PET, which can be measured using the Keyence VK-X3100. Supplementary Figure S8a or Figure S8b show a 2-D image of a hybrid TCE in an area where the material was removed, and a line cut is made to measure the step height. To smooth data for measuring step height, at least 10 lines in the direction perpendicular to the line cut are averaged, as shown by the green or blue area and trace in Supplementary Figure S8. The averaged line is shown in the X vs. Y plots of Supplementary Figure S8. Next, averages are taken at two locations, one across the bare PET and one across the hybrid TCE, as denoted by the red lines in Supplementary Figure S8b. Finally, the step height is measured as the difference between the average height of each red location. The average and standard deviation for the thickness of the hybrid TCE is determined by measuring at least five areas.

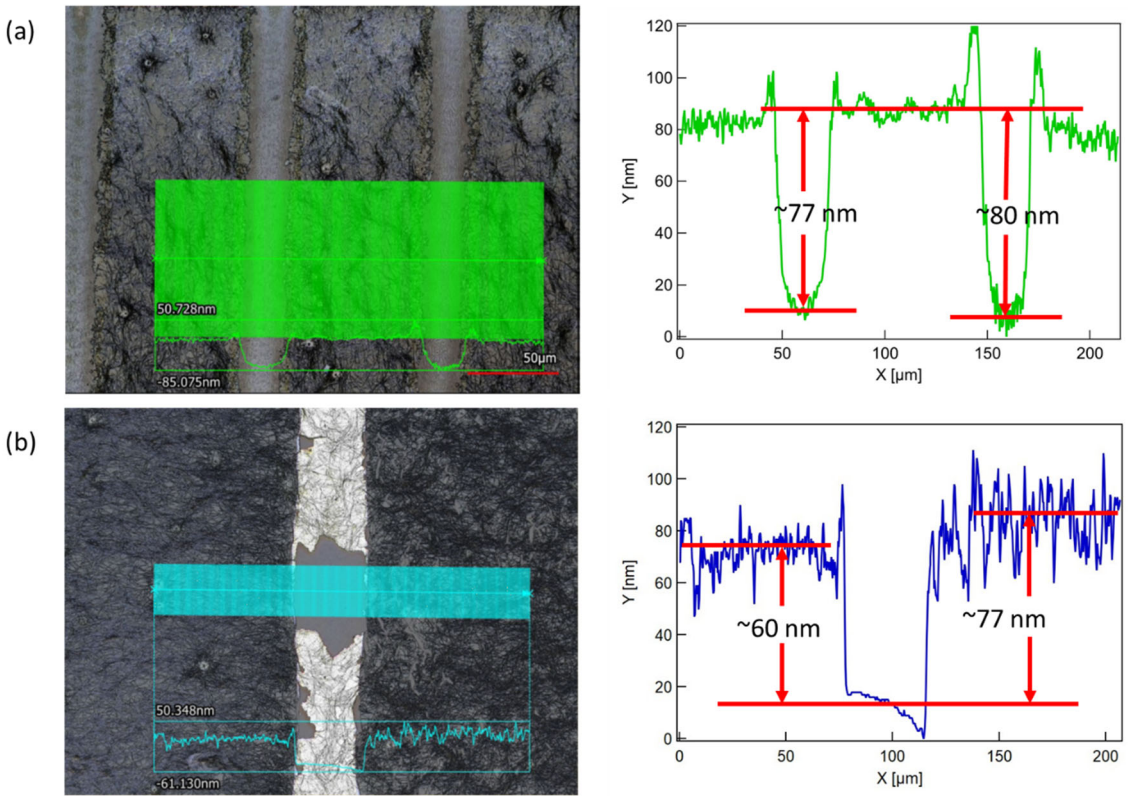

Figure S8. Hybrid TCE thickness measurements using Keyence VK-X3100: (**a**) Shows a 2-D image with the average height measurement shown by the green area on a hybrid TCE (made with the 9-pulse photonic curing condition) with material removed by laser cracking. An averaged line cut from the green area clearly shows the height difference between bare PET and hybrid TCE in the X vs. Y plot. (**b**) Shows the same process for a thickness measurement completed on a similar hybrid TCE by cracking and using scotch tape to remove material. The red lines indicate where data was averaged.

Voltage bias (~2 V) was applied to the PET/MBL substrate and the final hybrid TCE using a Keithley 2635B source meter, and the temperature rise due to Joule heating was imaged with an IR camera (TOPDON TC-001 connected to a Samsung S9 cell phone) to compare the current spreading characteristics of each sample. A schematic of each sample is given in Supplementary Figure S9a,d. When applying voltage bias on the PET/MBL substrate, copper tape/silver paint electrodes were applied along the long (down-web direction) edges of the sample to contact the Ag MBLs, as seen in Supplementary Figure S9b. Without the copper tape/silver paint electrode, the current won't flow through the Ag MBLs because they are not connected. Thus, if voltage was applied at the short (cross-web direction) ends of the sample, no heating was observed. When applying voltage bias on the hybrid TCE sample, alligator clips were attached at the short (cross-web direction) ends of the sample without copper tape or silver paint, as seen in Supplementary Figure S9c. Because the AgNWs are uniform across the hybrid TCE sample, no additional electrical connections were needed. Furthermore, the average AgNW coverage was measured to be (28 ± 5)% as calculated from SEM images of five samples. The SEM images (Supplementary Figure S10) were loaded into ImageJ and an area filter was used to calculate the percentage of AgNW area compared to bare substrate area.

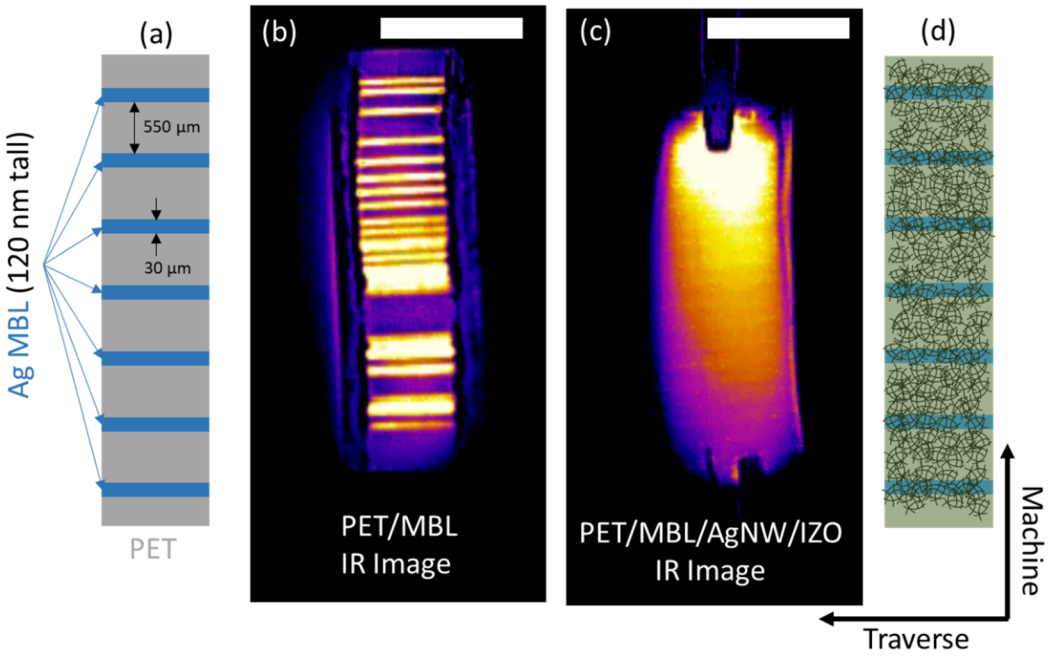

Figure S9. IR images of hybrid TCE: (**a**) PET/MBL substrate top-view schematic (PET in gray and Ag MBLs in blue), (**b**) IR image of a PET/MBL substrate under voltage bias applied to the long edges, (**c**) IR image of the hybrid TCE under voltage bias applied to the short edges, and (**d**) hybrid TCE top-view schematic (Ag MBLs in blue, AgNWs in black, and IZO in green). The voltage bias was ~2 V. The scale bars in (**b**,**c**) represent 1 inch.

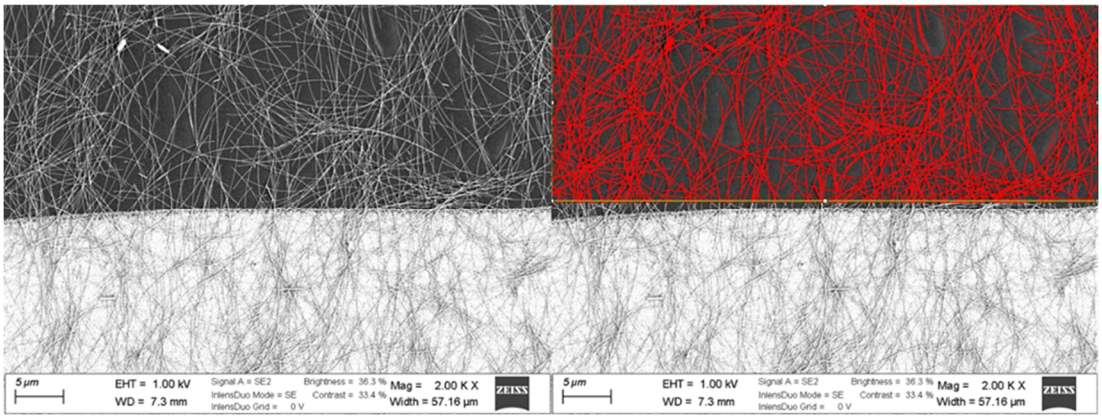

Figure S10. AgNW coverage: Representative SEM image of an AgNW-coated PET/MBL substrate at 2000x magnification before (**left**) and after (**right**) filtering the background using ImageJ. The analysis area selected was in the upper portion of the image (denoted by the thin yellow line and red colored AgNWs) to exclude the MBL feature. The red-colored AgNW area, as calculated from five different SEM images, was (28 ± 5)%.

To demonstrate the hybrid TCE can be conveyed over a 2-in roller in device fabrication using R2R without damage, we performed bending tests over 2000 cycles. The 1 in × 3 in sample is clamped between two crossheads (Supplementary Figure S11). The lower crosshead was fixed in position, and the upper crosshead can move. At the highest upper crosshead position, the sample is stress free, not under tension or compression. Then the upper crosshead is lowered to a 2-in gap between the crossheads, corresponding to approximately 1-in bending radius of the sample. The upper crosshead was cycled between these two positions repetitively. Two indium dots are placed at a 2-in separation on the TCE to monitor the resistance during the bending cycles.

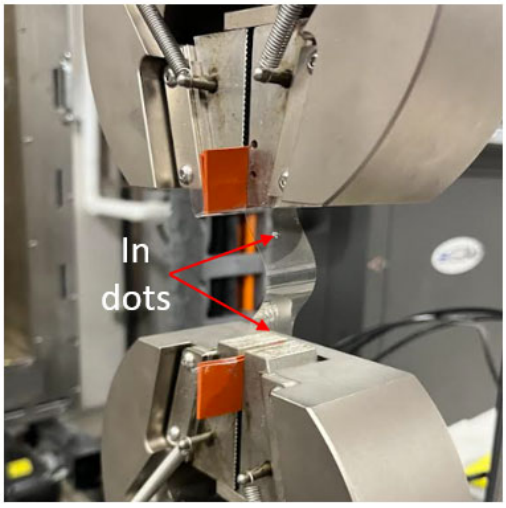

Figure S11. Bending testing equipment setup: Images of hybrid TCE sample clamped in bent position between upper and lower crossheads.

Scaling Up to Large Area

Pictures of large-area hybrid TCE samples being processed on the R2R photonic curing tool are shown in Supplementary Figure S12.

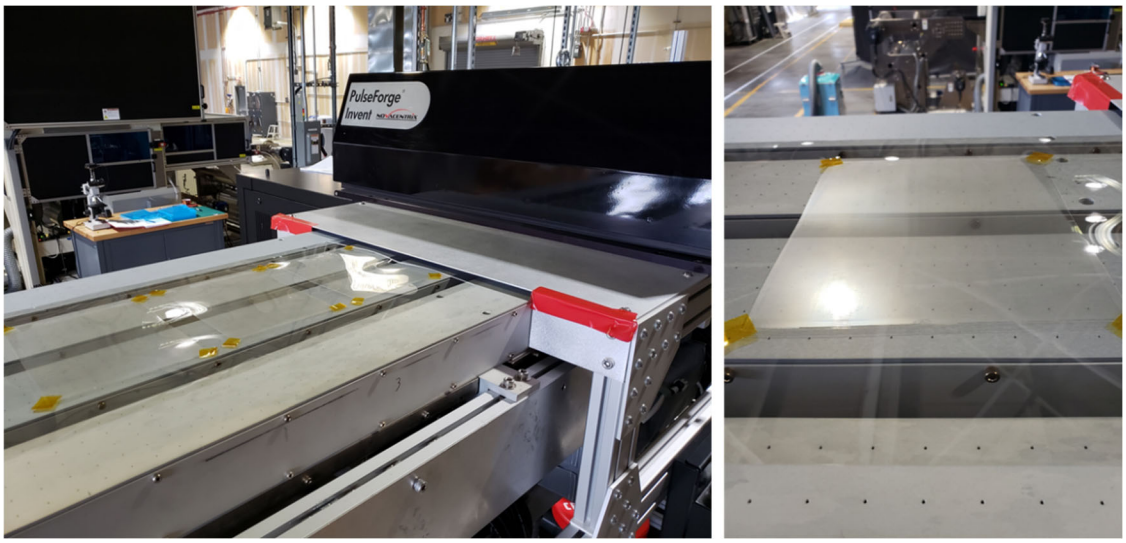

Figure S12. R2R photonic curing tool: Images of hybrid TCEs just after being conveyed through the R2R photonic curing tool. The flash lamp is enclosed in the black box, labeled PulseForge Invent, in the left image.

UV-Vis Absorption Spectra Similarity Analysis

Since the 9-pulse photonic curing condition produced high-performance hybrid TCEs, we wanted to find a 1-pulse photonic curing condition that would produce similar results. Thus, we used Latin Hypercube sampling (LHS) to generate photonic curing conditions (Supplementary Table S1) for processing hybrid TCEs using 1 pulse. We then measured their UV-vis transmittance spectra; the goal was to find the condition that produces a transmittance spectrum most similar to that of the sample made by the 9-pulse condition. To quantify the shape similarity between two transmittance curves, Procrustes analysis was used. Procrustes analysis is a metric of shape similarity, usually called the Procrustes distance, between a test curve and a reference curve [3]. The Procrustes algorithm rotates, translates, and scales the test curve seeking to minimize the average square distance between test and reference curves. In this way, differences between curves unrelated to curve shape are eliminated. A smaller Procrustes distance indicates a better match of the test data to the reference data. A representative UV-vis transmittance spectrum for a sample made using the 9-pulse photonic curing condition is shown in Figure 8a as the red curve and used as the reference. Each 1-pulse LHS photonic curing condition was tested, and the Procrustes distance was calculated for two to five repetitions of each condition. The transmittance data was smoothed to

eliminate measurement noise using cubic spline smoothing. Specific Procrustes values were calculated using the "Procrustes" function in Matlab for all LHS samples and repeats [4]. The lowest Procrustes distance calculated is reported in Supplementary Table S1 showing LHS4 has the smallest Procrustes distance. Some LHS photonic curing conditions burned the hybrid TCE and Procrustes distance was not calculated for those samples (LHS conditions 1, 2, 6, and 14). Based on Procrustes analysis, LHS condition 4 was determined to be the optimal 1-pulse photonic curing condition and used in the stitching processing. Normalized XPS spectra for Ag 3d, In 3d, and Zn 2p (Supplementary Figure S13a–c) also show similar results for hybrid TCE samples made by photonic curing with LHS condition 4 (1-pulse) or the 9-pulse condition.

Table S1. LHS conditions: 20 LHS conditions with specific photonic curing parameters and calculated Procrustes distance values.

LHS Condition	Lamp Voltage [V]	Fluence [J cm^{-2}]	Pulse Length [ms]	# Of Micro-Pulses	Duty Cycle [%]	Procrustes Distance [×10^{-3}]
1	420	4.8	7	13	45	-
2	425	4.4	11	10	25	-
3	380	3.0	16	27	20	1.42
4	330	3.6	10	24	65	0.568
5	315	4.0	21	19	65	0.900
6	485	4.8	6	21	35	-
7	305	3.4	29	17	40	1.07
8	260	2.4	18	8	55	1.26
9	240	1.8	24	3	30	2.22
10	230	1.8	23	15	50	1.78
11	290	3.2	27	5	50	1.32
12	270	2.4	13	28	60	1.94
13	220	1.6	29	4	40	3.54
14	370	5.0	12	18	65	-
15	300	3.2	20	14	50	2.61
16	450	2.6	6	30	25	1.51
17	355	2.5	8	30	30	5.14
18	315	2.5	10	29	45	4.54
19	250	2.2	27	5	45	5.85
20	400	1.8	8	30	20	5.57

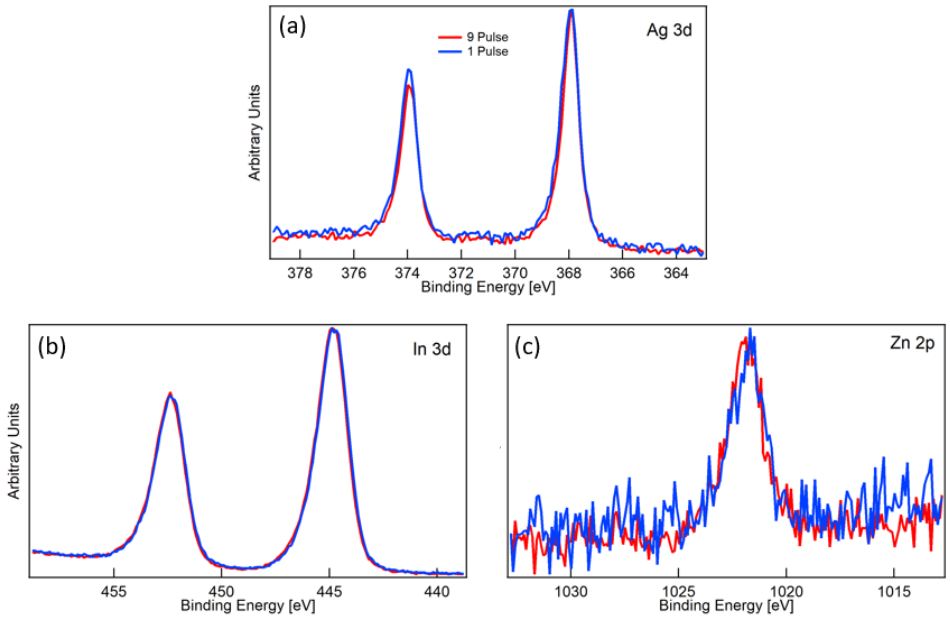

Figure S13. Normalized XPS spectra of hybrid TCE made with 9-pulse vs. 1-pulse: (**a**) Ag 3d, (**b**) In 3d, and (**c**) Zn 2p comparing the hybrid TCE made with 9-pulse photonic curing condition (red) and a hybrid TCE made with the 1-pulse photonic curing condition (blue).

Sample Preparation for 11 m per Minute Stitching Experiments

Because blade coating and photonic curing were performed at two locations 200 miles apart, stitching samples photonically cured at 11 m min^{-1} were made by blade coating two layers of IZO on top of AgNWs and dried at UTD. Then the samples were placed in a vacuum-sealed bag for transportation. Once the samples reached PulseForge, where the photonic curing tool with 15 kW power supply was located, the samples were taped to the stage with Kapton tape as in Figure 10, and photonically cured. After photonic curing, the samples were vacuum sealed again and transported back to UTD. The samples were rinsed with DI water before characterization and PSC fabrication.

Transmittance of Hybrid TCE with HTL

The transmittance after depositing each layer of the HTL on a hybrid TCE and SA PET/ITO is shown in Supplementary Figure S14a,b, respectively. The T_{avg} (referenced to air) of the hybrid TCE decreased from 79% to 74% after neutral PEDOT:PSS deposition. With an additional layer of PEDOT:PSS on top of the neutral PEDOT:PSS, T_{avg} decreased to 73%. Finally, adding MeO-2PACz on top of PEDOT:PSS lowered the T_{avg} to 71%. This shows that the primary reduction in T_{avg} is due to the initial neutral PEDOT:PSS layer.

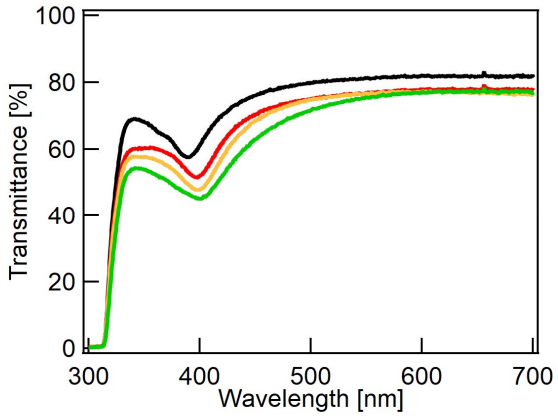

Figure S14. UV-Vis transmittance of hybrid TCE and HTL: The UV-Vis transmittance spectra of the hybrid TCE (black) after the sequential deposition of neutral PEDOT:PSS (red), neutral PEDOT:PSS/ PEDOT:PSS (orange), neutral PEDOT:PSS/ PEDOT:PSS/MeO-2PACz (green).

Comparing PSC Devices Made on Hybrid TCEs vs. SA PET/ITO

Supplementary Figure S15 and Supplementary Table S2 compare the performance of PSC devices made on hybrid TCEs vs. on SA PET/ITO. The HTLs for these devices are bilayer PEDOT:PSS/MeO-2PACz (4 mg mL^{-1}). For a fair comparison, PSCs on hybrid TCEs and PET/ITO were fabricated in the same batch.

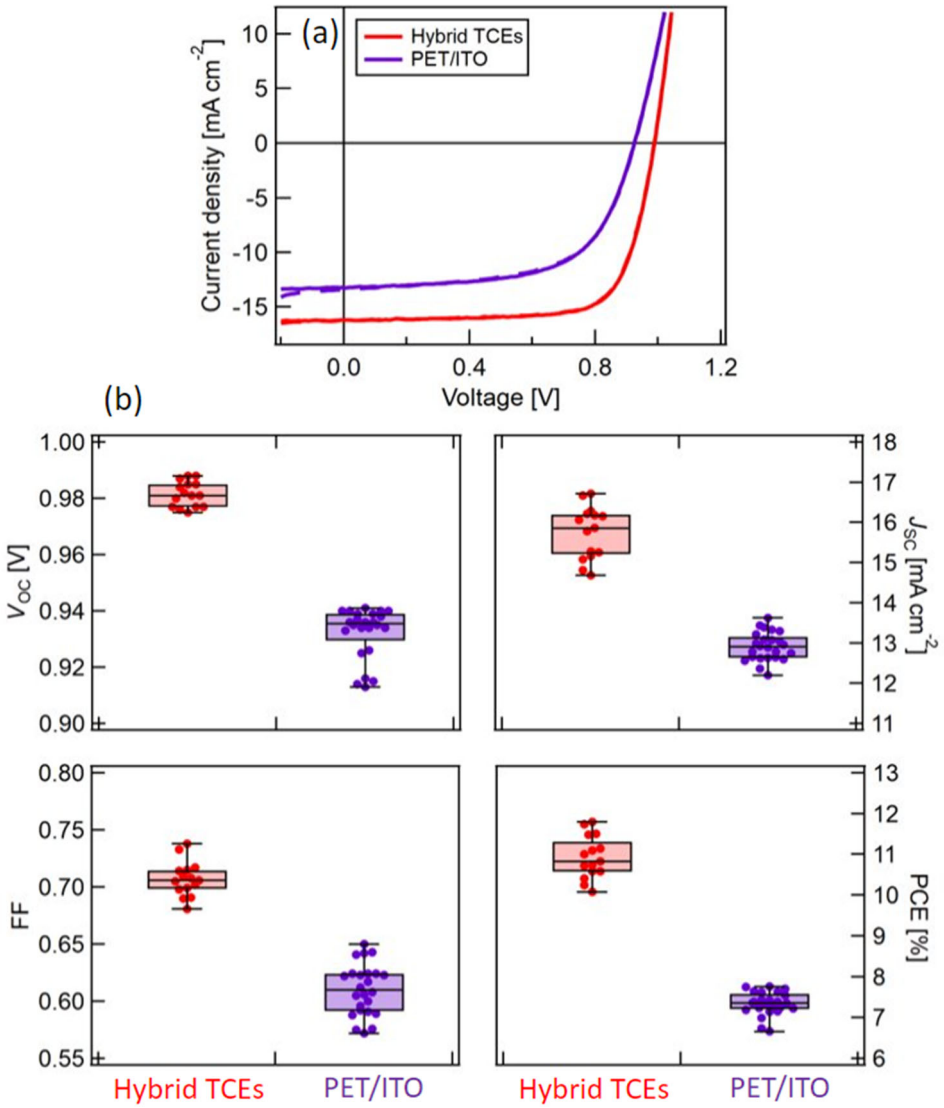

Figure S15. *J-V* results for hybrid TCE and PET/ITO: (**a**) Champion *J-V* forward and reverse curves and (**b**) Box plot comparing the average *J-V* parameters of the PSCs on hybrid TCEs (Red) and PET/ITO (Purple).

Table S2. Average *J-V* parameters along with champion PCE of the PSCs on hybrid TCEs and PET/ITO.

Substrate	Voc [V]	Jsc [mA cm^{-2}]	FF	Average PCE [%]	Champion PCE [%]
Hybrid TCEs	0.982 ± 0.01	15.7 ± 0.66	0.707 ± 0.02	10.9 ± 0.53	11.8
PET/ITO	0.932 ± 0.01	12.9 ± 0.35	0.610 ± 0.02	7.34 ± 0.28	7.65

PSC Devices on Stitching Samples

Forward and reverse *J-V* scans (Supplementary Figure S16) show low hysteresis for PSC devices made on stitching hybrid TCEs with the bilayer PEDOT:PSS/MeO-2PACz as HTL.

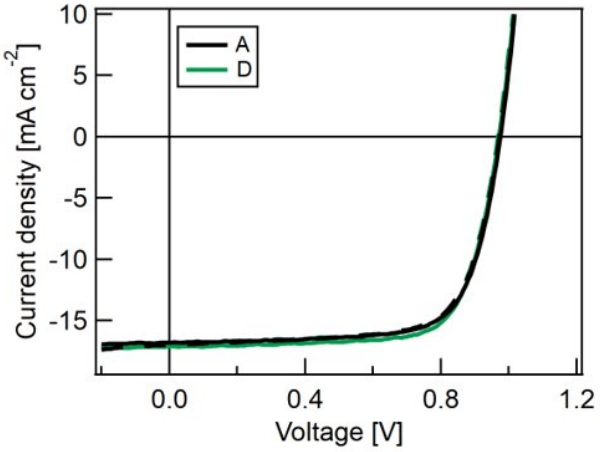

Figure S16. Champion PSC *J-V* curves for stitching samples: Forward (dashed) and reverse (solid) *J-V* scans for champion PSC made on hybrid TCEs placed at position A (black) and D (Green) during stitching photonic curing.

References

1. Sigma, M. Silver Nanowires 806714. Available online: https://www.sigmaaldrich.com/US/en/product/aldrich/806714 (accessed on 1 June 2023).
2. CheapTubes.com Silver Nanowires 30 nm OD. Available online: https://www.cheaptubes.com/product/silver-nanowires-30nm/ (accessed on 1 June 2023).
3. Gower, J.C. Generalized Procrustes Analysis. *Psychometrika* **1975**, *40*, 33–51. https://doi.org/10.1007/BF02291478.
4. MathWorks Procrustes. Available online: https://www.mathworks.com/help/stats/procrustes.html (accessed on 1 June 2023).